Influence and Effectiveness of Water-Repellent Admixtures on Pozzolana-Lime Mortars for Restoration Application

Laura Falchi[a*], Urs Müller[b], Patrick Fontana[c], Francesca C. Izzo[a], Elisabetta Zendri[a]

[a] Department of Environmental Sciences, Informatics and Statistics, Ca' Foscari University of Venice
Via Torino 155/B, 30172 Venice Mestre, Italy
laura.falchi@stud.unive.it, Fra.izzo@unive.it, elizen@unive.it

[b] Swedish Cement and Concrete Research Institute
Brinellgatan 4, SE-504 62 Borås, Sweden
urs.mueller@cbi.se

[c] BAM, Federal Institute for Materials Research and Testing, Division 7.1 Building materials
Unter den Eichen 87, 12205 Berlin, Germany
patrick.fontana@bam.de

[*]**Corresponding Author.**
Laura Falchi,
Department of Environmental Sciences, Informatics and Statistics, Ca' Foscari University of Venice
Via Torino 155/B, 30172 Venice Mestre, Italy
laura.falchi@stud.unive.it
Telephone: 0039 041 234 6732; 0039 041 234 6730
Fax: 0039 041 234 6729

Article type. Research paper

Abstract

Pozzolana- lime mortars modified with water-repellent admixtures were designed and studied to obtain mortars for restoration application. Powdered silane and calcium stearates were mixed with pozzolana, lime and sand and the chemical-physical properties of the resulting mortars were evaluated by X-ray diffraction, electron microscopy (SEM-EDX), thermogravimetric analysis and FT-IR spectroscopy. The mechanical behavior, the pore structure and the hygric behavior were measured.

The resistance of water-repellent mortars to the salt crystallization was evaluated. Both calcium stearates and powdered silane allowed good water-repellent protection even if the water-repellent agents and their dosage modified some physical properties and the hydration kinetic.

Keywords: water-repellent admixtures, pozzolana- lime mortars, water absorption, hydration, stearates, silane, restoration

1. Introduction

Hydraulic lime mortars are defined as mortars capable of setting and hardening by chemical reaction with water in humid and wet environment. Although hydraulic lime and hydraulic lime mortars are described by EN 998-1 and EN 459-1, EN 459-2, EN 459-3 [1,2], the first use of volcanic sands in mortars seems to be dated back to the 10th century B.C. when Phoenicians mixed natural pozzolana in water engineering structures and ports [3]. Greeks used to add some volcanic pozzolanas from Santorini to their mortars, and then through Romans the use of pozzolanas in mortars became a well-regulated practice [4]. A similar hydraulic effect could be obtained also by substituting ordinary sand with finely ground bricks or tiles: this technique was commonly used in Venice since the 14th century A.D. for rendering mortars, plasters, mosaics, frescoes and floors in "Venetian style", thanks to the good resistance of these mixtures in the wet/salty climate of the lagoon [5,6]. But from the 19th century Portland cement gained more and more a position of predominance replacing natural cements [7]. In the last century cement-based materials have been often used also in restoration treatments for historical buildings. However, nowadays the conservation scientists agree that cement is not always the best solution for repairing and restoring ancient constructions [8] because the mechanical, microstructural and chemical properties of cement mortars often differ from the ones of the historical building materials [9].

In the field of conservation the requirements of adopting compatible, reliable, durable solutions (able to repair ancient and historic structures without causing any new damages), leads to rethink on the use of cement mortars and to prefer natural hydraulic lime mortars or pozzolana-lime mortars. These kinds of mortars demonstrate better chemical, mechanical and microstructural characteristics compatible

with several traditional building materials and historical mortars [10-12]. In the last years scientific interest in lime-based mortars has increased and different studies have focused in particular on the use and the properties of pozzolanas in hydraulic lime mortars [13-15].

The above mentioned, compatible, pozzolana-lime mortars show a better durability in moist environments in comparison to aerial lime mortar [16], they are however wettable and usually present a higher capillary water absorption in comparison to cement mortars. This means that also pozzolana-lime mortars can be exposed to the most severe deterioration factors which could affect their durability due to the damaging action of water: wet and dry cycles, weathering/rain exposure, freezing and thawing cycles, exposure to salt solutions [17]. To enhance the capabilities of these mortars to protect the surfaces of historical architectures from the damaging action of water or of salt solutions, it is possible to use water-repellent admixtures, analogue to the use in cement mortars [18-21].

In the presented study water-repellent hydraulic lime mortars made with hydrated lime, Greek natural pozzolana, sand and water-repellent admixtures were prepared and studied. The purpose of investigation was: i) the evaluation of the influence of hydrophobising additives on binder hydration reactions, ii) the influence on the microstructure and porosity of the mortars, iii) the resistance of the water-repellent mortar to moisture and salt crystallization.

In a series of preliminary tests different water-repellent admixtures, i.e. sodium oleates, zinc stearates, silane emulsions, calcium stearates (commonly used to obtain water-repellent cement mortars) and powdered silanes/siloxanes [22-24] were evaluated. Even if in some studies the better water repellence performance of calcium oleates compared to calcium stearates was reported [25], the preliminary tests showed that with oleate workability, setting, and mechanical properties of the mortars were negatively affected compared to calcium stearates and the powdered silanes/siloxanes. Therefore these products were studied in detail and the results are presented in this paper.

The use of instrumental techniques such as X-ray diffraction (XRD), scanning electron microscopy with energy dispersive X-ray spectroscopy (SEM-EDX), Fourier-transform infrared spectroscopy (FT-IR), thermal analysis (DTA-TG), and different tests to evaluate mechanical and physical properties of the mortars allowed studying the different water-repellent systems and the influence of the additives

on the systems' properties. Moreover, the effect of salt crystallization on the water-repellent mortars was studied [26, 27], in order to evaluate their durability towards salt attack.

2. Materials and methods

2.1 Starting materials

A mixture of industrial lime hydrate and a pozzolana of volcanic origin from Greece was used as binder system. The lime was a pure calcium hydroxide ($Ca(OH)_2$) supplied by BASF®. The pozzolana was the S&Bμ-silica®, a buff coloured volcanic ultrafine siliceous material with a high glass content supplied by S&B Industrial minerals. CEN standard sand defined by EN 196-1 [28] was chosen as aggregate (siliceous sand with a size fraction of 0/2). Two different kinds of water repellent products were chosen: 82 % pure calcium Stearate purchased from Sigma Aldrich as a mixture of calcium stearates-palmitates and other fatty acid; Silres A® purchased from Wacker Chemie®, a silane/siloxane supported on silica powder (henceforth named simply 'silane').

Dry powder samples of the starting materials were characterized via X-ray diffraction (XRD) and X-ray fluorescence (XRF) analysis. The XRF analysis was carried out with an EDAX EAGLE III instrument, with a X-ray tube at 40 kV (Rh), 80 mm^2 nitrogen cooled lithium-drifted silicon crystal detector. EDAX Data Acquisition Module via PCI interface was used to acquire and process the data. The XRD measurements were done with a Rigaku Ultima IV X-ray diffractometer(40 kV and 40 mA Cu X-ray tube). The measurements ranged from 3° to 63° 2θ with a 0.02° 2θ step size.

2.2 Water-repellent pastes and water repellent mortars

Two different kinds of samples were prepared and studied:

- binder pastes mixed with water-repellent admixtures allowed to study the hydration reactions of the pure binder in presence of water-repellent agents;
- mortar mixes made of pozzolana-lime binder, sand and water-repellent admixtures allowed to evaluate the physical-chemical performances of water-repellent mortars and the resistance to salt crystallization.

2.3 Study of the hydration reactions of pozzolana-lime pastes

Binder pastes were prepared by mixing calcium hydroxide and pozzolana by a mass ratio of 1:1. The water-repellent admixtures were added at 1% by mass of the binder, while water was added in a water to binder (w/b) ratio of 0.8. The same w/b ratio was used for the mortars, as described below. The dosage of the water-repellent admixtures was chosen considering previous literature data and the necessity of having enough admixtures to observe possible effects [18, 21]. One mix was prepared without admixture and was used as reference. The mixes were stored in closed PET vessels at 23°C. Samples were collected at different hydration times (0, 2, 4 hours; 1, 2, 7, 14, 21, 28, 42, 56, 84, 140 days) and dried in a vacuum oven at 40 °C and 40 mbar for 7 hours to stop the hydration processes. The samples were then stored under nitrogen atmosphere to avoid carbonation.

Different analyses were performed to observe the formation of hydration products to better understand the setting and hardening mechanisms involved when the selected pozzolana is mixed to calcium hydroxide, and how the presence of water-repellent admixtures can influence the hydration reactions of this system.

Qualitative XRD powder analysis was performed on dried and ground samples. The same measurement parameters were used as for raw-material characterization.

SEM-EDX observation was carried out on fractured surfaces using a Philips Quanta 200FEI instrument with a Tungsten cathode and a Si(Li) Brucker 133 eV EDS detector.

The TG-DTA analyses were performed on powdered samples at 0, 2, 7, 28 days of hydration. The samples were ground and measured with a Netzsch STA 409/C instrument in alumina crucible, a heating program of 10 °C/min from 20 °C to 1000 °C in N_2 atmosphere was used.

A Perkin Elmer Spectrum One FT-IR ATR with diamond cell was used to measure the transmittance in the 500-1400 cm^{-1} range, with 1 cm^{-1} resolution and 32 scan/sample on ground samples collected at 0, 7, 28, 84 days.

2.4 Physical-chemical characterization of water-repellent mortars

Water-repellent mortars were prepared by mixing pozzolana and calcium hydroxide in a ratio of 1:1 by mass and a mass ratio of 1:7 (1:3 by volume) binder/aggregate was used. The different admixtures were added at 0.5 %, 1 %, 1.5 % of the total dry mortar's weight. These three different percentages were chosen considering previously published data in order to evaluate the influence of different

dosage on the mortars performances, beside the different nature of the water-repellent admixture [18, 21]. Mortars prepared without water-repellent admixtures were used as reference mixes.

The materials were mixed with water in a planetary mixer for 10 minutes, to allow a homogeneous distribution of the different components. The amount of water was adjusted in order to achieve a mortar slump flow of (170±10) mm with the flow table test according to EN 1015-3 [29]. The bulk density of the fresh pozzolana-lime mortars was measured following UNI EN 1015-6:2007 [30].

On two fresh samples of each mixture the setting time with the Vicat's needle method (UNI-EN 196-3) [31] was determined at 20 °C. The other fresh mixtures prepared were poured in oiled 4X4X16 cm moulds (a veil of oil was necessary to allow the de-moulding of the mortar samples) , and then placed in a curing chamber at RH = 90 % and T = (23 ± 2) °C for 28 days.

The physical-chemical characterization of water-repellent mortars after 28 days of curing included the evaluation of the density and microstructure, the evaluation of the mechanical strength and the evaluation of the behaviour of water-repellent mortars in the presence of water. The test performed completely characterized the systems, obtained interconnected data, and allowed a full understanding of the effects of the added water-repellent admixtures on lime-pozzolana mortars. For all the tests, the average of the results of three specimens for each mixture was considered.

The bulk density of the hardened mortars was calculated on dried prismatic specimens considering the ratio between their masses and their apparent volumes, while the real density was measured with a helium pycnometer on ground samples (particle diameter < 63 μm). With mercury intrusion porosimetry (MIP) the bulk density, the total open porosity and the pore size distribution were measured. MIP analysis was performed on samples collected from the bulk of 28 days-aged mortars as described in the Normal 4/80 [32] using a Pascal 140 and a Pascal 240 Thermo Quest/Finnigan instruments, able to measure minimum pore radii of 3.7 nm.

Mechanical tests were performed on 28 days aged mortars according to UNI EN 12390-3:2009 and UNI EN 12390-5:2009 [33,34]. A Zwick/Roell Z010 press was used with a pre-load of 10 N and a loading rate of 5 N/s for the flexural strength, and a pre-load of 20 N and a loading rate of 50 N/s for the compressive strength evaluation. The Testxpert II software was used for data elaboration. The

curves of load versus strain were registered, the elastic modules were calculated with the tangential and the secant methods.

Capillary water absorption tests were performed according to the procedure described in EN 1015-18:1999 in a climatic chamber at (23 ± 2) °C [35]. Cube specimens (40 mm^3) were cut from the mortar prisms with a diamond saw after 28 days of curing. Water absorption tests were performed through the cut face of the cubes and not through the moulded face in order to avoid an influence of the de-moulding oil. The water vapour permeability was evaluated following UNI EN 1015-19, DIN 52615 and DIN 52752 [36, 37]. The water vapour transmission and the water vapour resistance factor μ were calculated.

2.5 Determination of resistance to salt crystallization

The resistance to salt crystallization was evaluated according to EN 12370 [38]. The specimens were immersed in a saturated salt solution of sodium sulphate decahydrate for immersion cycles of two hours, followed by drying at 40 °C for 22 hours in the oven. The mass loss was measured after each cycle.

To evaluate the depth reached by the salts, after the test the degraded specimens were cut and samples collected every 0.5 mm from the outer layer to the inside of the specimen. The evaluation of the soluble salt content in each of these samples was done by measuring the ionic conductivity as described in the Normal 13/83 [39].

Capillary water absorption measurements were repeated on the degraded specimens after salt extraction/desalination in deionised water.

3. Result and discussion

3.1 Composition of mortar constituents

The XRF analysis of the calcium hydroxide showed, as expected, a high percentage of calcium, while low amounts (minor of 1 % in oxides) of sodium, silicon and magnesium have been registered (Table 1). The XRD analysis (Figure 1) detected the presence of portlandite ($Ca(OH)_2$) and a minor presence of calcite ($CaCO_3$) due to a slight carbonation.

The pozzolan appeared to be composed mainly of silicates and alluminates. The XRD pattern (Figure 1) shows a broad peak from 16° 2θ to 32° 2θ due to the presence of amorphous compounds such as

volcanic glass. Quartz (SiO_2), feldspar and the clay minerals illite and halloysite were the major crystalline phases, but other alumo-silicates were likely present in lower amounts. From the XRF analysis of the water-repellent admixtures (see Table 1) a high amount of silicon in the silanes and a high percentage of calcium in the stearates was observed. The XRD spectrum (Figure 2) of the silane presents broad peaks due to the amorphous silica, while calcium stearate was crystalline and showed complex XRD patterns in which metallic stearates and palmitates were recognizable.

3.2 Study of the hydration reactions of pozzolana-lime pastes

XRD patterns of the reference binder paste HLA, without water-repellent admixtures, obtained at different times of hydration were compared (Figure 3). Portlandite, quartz, albite were easily recognized and due to the presence of lime and pozzolana. However, the main difference in the XRD patterns can be seen at low angles (8-13° 2θ in Figure 2 and Table 2), where the main peaks of AFm in form of monocarbonate and C-A-S-H phases were found. At early stages, the XRD pattern of HLA presented the peaks related to the halloysite $Al_2Si_2O_5(OH)_4.2H_2O$ (peak 1 at 8.9° 2θ), but after 1 day of hydration halloysite peaks decreased and a new peak at 11.36° 2θ appeared (labelled as 2): halloysite was consumed to form monocarbonate AFm solid solution (peak no.2). After 7-14 days instead of the AFm solid solution two different modifications of AFm phases were identified at 11.2° 2θ and 11.42 2θ (peaks no. 2 and no. 3): Para-aluminumhydrocalcite Ca $Al_2(CO_3)_2(OH)_4.6H_2O$ (peak no. 2) and calcium aluminium oxide carbonate hydroxide hydrate $Ca_4Al_2O_6(CO_3)_{0.5}(OH).11.5H_2O$ (peak no. 3). After 5 months it was possible to observe another small peak at 11.75° 2θ, identified as a Calcium aluminium oxide carbonate hydrate ($Ca_4Al_2O_6.CO_3.11H_2O$). Similar compounds have been previously found in aluminate cements and in studies on the hydration of C_3A phases also in presence of $CaCO_3$ [40-45]. Furthermore, it was observed the decrease of the broad reflex of the volcanic glass in the range of 20-35° 2θ during the curing and the increase of a broad peak in the range 3-10° 2θ due to the formation of new amorphous hydrate phases, together with the increase of a broad peak centred at 29° 2θ, due to the formation of C-S-H. When water-repellent admixtures were added, the mechanism of reaction remained the same and similar products were observed, but some differences in the reaction kinetic occurred (Figure 3 and Table 2). For the paste HLcas1, with calcium stearate, the peak no. 2 of AFm solid solution at two days was broader and lower than in HLA; after 140 days the peak no. 4

(Calcium Oxide Carbonate Hydrate $3CaO.\ Al_2O_3CaCO_3.11H_2O$) was not detected. The paste HLsil1, with the silane showed a similar reaction rate to HLA. This type of water-repellent admixture seemed not to strongly influence the hydration reaction.

SEM observations of the sample showed the formation of denser, gel-like structures during the hydration (Figure 4). EDX analyses showed high presence of aluminium and carbon on some elongated grains, while silicon was mainly detected on the gel-like structures bonding the grains. The latter observation confirmed the formation of amorphous C-S-H, which was well developed in HLsil1 at 28 days, in HLA after 56 days and in HLcas1 after 84 days; furthermore an overall denser structure and a dense network of hydraulic compounds were observed for the pastes HLsil1 already after 28 days. For HLcas1 a similar structure as for HLA was observed.

TG- DTA technique allowed to obtain quantitative data about the chemical composition. HLA, HLsil1 and HLcas1 were analyzed as fresh paste, and after 2, 7 and 28 days. The results of the analysis are displayed in Table 3 and Figure 5. The total bound water (Tbw), due to different dehydration reactions of silicates and aluminate hydrates, was considered in the temperature range of 100-350 °C. The dehydration of calcium hydroxide ranges from 400 °C to 550 °C and the decarbonation of $CaCO_3$ from 650 °C to 800 °C. The increase of the Tbw and the decrease of the calcium hydroxide during the hydration were clearly visible due to the formation of amorphous aluminate and silicate hydrates. The calcium carbonate content was low and varied randomly from sample to sample. Only slight differences were observed for the different mixtures regarding their composition at same hydration times. Mixture HLsil1 had the lowest amount of $Ca(OH)_2$ after 28 days in comparison to mixture HLA, while mixture HLcas1 had the highest one. The powdered silica-silane additives aided the hydration of HLsil1 possibly by pozzolanic reaction of the silica substrate, while the calcium stearates seemed to slow down the hydration rate of HLcas1.

The FT-IR measurements confirmed the presence of the aforementioned hydration compounds (Figure 6). The major peaks visible in the fresh samples spectra were due to the calcium hydroxide (–OH stretching at 3636 cm^{-1}) and due to the silicates (Si-O-Si stretching at 1100-900 cm^{-1} but centered at 1020 cm^{-1}). The peaks at 1431 cm^{-1} and 788 cm^{-1} indicated a minor amount of calcium carbonate. The broad absorption at 1431^{-1} cm was also due to double CO_3^{2-} stretching absorptions of the allumino-

carbonate phases. While the hydration proceeded the silicate peaks changed shape and became broader. After 7 or 28 days it was possible to distinguish a second silicate peak around 955 cm^{-1} due to the presence of different calcium silicate hydrates (C-S-H). The presence of this peak clearly showed the formation of gel-like, amorphous, C-S-H phases, not detectable by XRD analyses. The different pastes showed very similar spectra. The only differences were observed for the mixture HLcas1, which presented two peaks of aliphatic stretching at 2917 cm^{-1}, 2840 cm^{-1} associated with calcium stearates. No big differences for the different mixtures were seen also over time. A slightly different displacement of the hydrated silicates peak at 955 cm^{-1} was observed, in particular the 955 cm^{-1} and 1020 cm^{-1} peaks intensity ratio versus the curing time increased faster for HLsil1, showing a faster consumption of anhydrous silicates to form C-S-H in the first days (Figure 6b). However, after 84 days, no differences were observed.

The presence of silane/siloxanes caused a faster formation of gel-like C-S-H after 28 days in HLsil1 as evident by SEM observations. It is possible that the silica carrier grains had an additional pozzolanic effect similar to silica grains in cement pastes [46, 47], which enhanced the production of amorphous C-S-H instead of crystalline carbonate-aluminates. However, a slight delay of the entire hydration was assumed due to the absence of a preponderant peak at 950 cm^{-1} after 84 days in FT-IR analysis and by lower Tbw and higher $Ca(OH)_2$ contents found with TG-DSC measurements. Probably the product was adsorbed on the pozzolana surfaces creating an hydrophobic barrier which prevented a normal hydration.

The hydration delay observed in HLcas1 samples was probably caused by an ion exchange and adsorption of the long hydrophobic chains of stearates/palmitates on pozzolana and calcium hydroxide as reported in [24, 48, 49]. In pozzolana-lime pastes, the dissolution of calcium carbonate covered by hydrophobic stearates into the reaction solution might be prevented and the whole pozzolanic reaction proceeded slower.

3.3 Physical-chemical characterization of water-repellent mortars

3.3.1 Fresh mortars

Table 4 summarizes the composition of the different mortars and the fresh mortar properties. The pozzolana-lime mixtures at a ration 1:1 by mass constituted the binder, and the w/b ratios ranged from 1.13 to 1.30 in order to obtain a good workability. HLcas mixtures, with calcium stearate, required a higher content of water in order to get the required workability. Also the density of fresh mortars was influenced by the water-repellents: the mixtures HLCas presented lower density in comparison to the mixtures HLA and HLsil. A long setting time was observed: 35 hours for the reference mixture HLA and even more when calcium stearate or the silane were added; the addition of water-repellent admixtures delayed the setting. This delay is explained by the adsorption of the hydrophobic compound on a part of the the binder grains which delayed the hydration reactions as explained in the previous section.

3.3.2 Hardened mortars

The density and porosity data (displayed in Table 5 and Figure 7) allowed understanding the mortar's microstructure. It was observed that the bulk density was strongly influenced by the presence of the admixtures. The reference mixture HLA had the highest apparent density and a total porosity of approx. 32 %. The addition of silanes (mixtures HLsil0.5, HLsil1, HLsil1.5) caused the decrease of density, due to the formation of air bubbles inside the system acting as an air-entraining agent. The mixtures HLcas0.5-1-1.5 and HLA had similar densities and similar total porosities (33-34 %). The addition of stearates seemed, therefore, not to have changed the air content of the samples. In every case differences in the dosage of water-repellent admixtures did not influence significantly the apparent density. MIP analysis revealed a bimodal distribution of the pore sizes for all mixtures, but the curves of the relative pore volume differ in the location of the peaks: i) peaks at 0.1 µm and at 9 µm for HLA and HLcas1; ii) peaks at 0.06 µm and 9µm for HLsil1.

These differences in the relative density of mortars are only partially reflected by their mechanical properties. In Table 5 the results of the mechanical tests are displayed. The compressive strength at 28 days of the reference mortar HLA was 2.0 MPa and the flexural strength was 0.37 MPa in average; values that have been commonly observed with this kind of hydraulic lime mortars [50, 52]. It was observed that the mechanical performance of the mortars changed slightly depending on the admixture used. The addition of both the silane and calcium stearate (mixtures HLsil and HLcas) led to similar

strength values of approx. 2 MPa for compression strength and 0.4 MPa (HLcas) and approx. 0.3 MPa (HLsil) for flexural strength at 28 days.

The strength values of HLcas mixtures were slightly higher than those of the HLsil mixtures, due to their compactness (as confirmed by the lower porosity and the higher apparent density of HLcas mixtures). Regarding the admixture dosage, the higher the percentage of the silane was, the better was the compressive strength of HLsil mixtures with values ranging from 1.73 MPa for 0.5 % of admixture to 2.04 MPa for 1.5 % of admixture. For calcium stearate the strength decreased with increasing addition.

The study of the behavior of water-repellent mortars in relation to liquid water was a focal point of this research. This behavior was evaluated by capillary water absorption tests. The capillary water absorption coefficients are reported in Table 6. Specimens of HLA had a high capillary water absorption coefficient C. The addition of the silane (mixtures HLsil0.5-1-1.5) resulted in very low absorption coefficients. Calcium stearate seemed to lower the water uptake of the mortar specimens only at higher concentrations (mixture HLcas1.5) (see also Figure 8).

The water vapor permeability had also to be taken into account because most of the historical mortars have high water vapour permeability: a suitable mortar for the reparation and restoration of historical buildings should have a good permeability to be compatible. One of the mostly used and simple indicator of the breathability of a porous substrate is the water vapor resistance factor (μ). Cement mortars usually present μ values in the range of 15-35 and more, while cement-free hydraulic mortars are characterized by a higher permeability and a vapor resistance factor that can vary in the range of 4-15 [21, 53]. The water vapor permeability of the samples is linked to the mortar structure, but can be also influenced by the water-repellent admixture. The water vapor permeability measured for the different mixtures are listed in Table 6. HLA presented a μ value of 11±1 whereas for mixtures HLsil and HLcas, higher μ values were found. Increasing the dosage of admixtures from 0.5 % to 1.0 % and 1.5 % caused a reduction of the permeability for the mixtures HLsil and HLcas.

3.4 Determination of resistance to salt crystallization

Figure 9 shows images of the specimens before and after the salt resistance tests and the mass losses during the cycles. The specimens HLA and HLcas presented serious degradations after a few cycles,

and it was impossible to repeat more than five cycles because the complete disintegration of HLA specimens occurred. Specimens of mixtures HLA and HLcas0.5 presented a mass loss of 30-40 % after 5 cycles. When higher amounts of calcium stearates were added (mixtures HLcas1 and HLcas1.5), the resistance to salt degradation increased and lower mass losses were measured. The degradation of HLA, HLcas0.5, HLcas1, and HLcas1.5 proceeded with the disaggregation of the outer layers and in some place of HLcas1 also spalling and delamination of the surfaces occurred (Figure 9). The presence of the silane, even with only 0.5 %, was much more effective against the degradation due to salt attack. Only small changes were observed with slight mass losses (Figure 9).

The ionic conductivity measurements performed on samples of mixtures HLA, HLsil1 and Hlcas1 allowed to understand the salt distribution inside the different matrices (Figure 10 and Table 7). After salt crystallization mixtures HLA and HLcas1 showed higher conductivities, in particular in the outer part of the specimens (0.5-0 cm) reaching values of 200-250 µS/cm. The salts were, however, able to deeply penetrate the specimens of mixtures HLA and HLcas with conductivities of around 130 µS/cm also in the specimen cores (2.0-1.5 cm). HLsil, however, did not show a significant increase of the conductivity after the salt cycles and the conductivity remained constant over the entire profile of the specimens.

After the cycles, the water absorption coefficient of the samples was measured again (Table 4). However, HLA specimens were completely disintegrated and it was not possible to test them. The water absorption of mixture HLsil0.5 increased slightly, but with higher dosages of the silane (HLsil1, Hlsil1.5) the absorption diminished. To explain the lower capillary absorption of these two mixtures, it has to be considered that during the immersion the water might improve a further hydration of the mortars, leading to higher compactness of the external layer. The low capillary absorption can explain the good resistance of these mixtures against salt crystallization because the salts were not able to penetrate and crystallize inside the samples, as was confirmed also by the ionic conductivity measurements. HLcas mixtures presented higher water absorption coefficients after the salt test. In particular, HLcas0.5 and HLcas1 reached values around 60 g/($m^2s^{0.5}$) losing their water repellence properties, while the coefficient of HLcas1.5 increased to 29 g/($m^2s^{0.5}$).

The week hydrophobic effect of the mixtures containing calcium stearate affected their resistance to salt crystallization: the salt solution was able to penetrate from preferential points and salt crystallized underneath the surface causing spalling. It is assumed that the non-optimal water repellency was due to different reasons such as inhomogeneous distribution of the calcium stearate in the binder matrix, formation of calcium stearates lumps/deposits inside the bulk, preferential disposition of this products on the external surfaces [25, 54]. A second reason might have been an ionic exchange with calcium ions in the system that led to the attachment of the stearate chains to calcium carbonate grains in the initial stage of hydration, which then were partially covered by wettable hydration products resulting in the decrease of the water repellency of the system [24].

4. Conclusions

In this study water-repellent mortars were designed suitable for restoration works at historical buildings. The composition of the mixtures was tailored considering the compatibility of these new mortars with ancient traditional mortars.

Therefore, a mix design similar to historic compositions was developed based on a natural pozzolana-lime binder. Hydraulic lime mortar with a binder composed of pozzolana and lime has been prepared because this composition reflects the traditional composition of several historical mortars. Furthermore, new water-repellent admixtures were added to the mixes in the attempt to improve their durability and their resistance to the damaging action of water and salt solutions. Several tests were performed to evaluate their properties.

Through the physical-chemical study of both water-repellent pastes and mortars, it was possible to understand how deeply their properties were influenced by the presence of water-repellent admixtures. The nature of the admixtures and, in second place, their dosage modified the whole properties of the mortars affecting, sometimes dramatically, the setting time, the mechanical strength, the microstructure, the permeability of the mortar and the capillary water absorption.

When the silane was used, the hydration reactions were not influenced but the setting time was increased. The physical properties, however, slightly changed. Good water-repellent performances were observed. The dosage used seemed not to seriously affect the properties of the hardened mortars and no big differences were observed by changing the dosage from 0.5 % to 1.5 % by mass.

The calcium stearates seemed to slightly slow down the hydration reactions but a good mechanical strength was observed. An optimal water repellence was obtained only with a higher dosage.

The second part of this paper addresses the problem of the resistance of the mortars to salt crystallization. The complete wettability of HLA specimens together with the limited mechanical performance resulted in a fast decay of the samples. When the silane was added to the mortars the resistance to salt crystallization was strongly enhanced due to the complete water-repellent effect obtained with this admixture.

The work done on laboratory specimens allowed to evaluate the general physical and chemical characteristics of pozzolana-lime water-repellent mortars. However, further investigation in laboratory and in field conditions, with application of mortars on salty masonry might be done in order to test the suitability of the designed mixtures for restoration of historical buildings in particular environments. In particular a possible application in the difficult testing ground of salty masonries in Venice might be a possible and desirable future perspective of this work.

Acknowledgments

The authors wish to thank Mr. André Gardei for mechanical testing, Ms. Elgin Rother for performing MIP analyses, and Mr. Klaus Oppat for performing TG-DTA analyses.

References

[1] EN 998-1:2003. Specification for mortar for masonry.-Part 1: rendering and plastering mortar. European Committee for Standardization.
[2] EN 459-1:1996, EN 459-2:1996, EN 459-3:1996 . Building lime. Part1: Definitions specifications and conformity criteria, Part 2 Test Methods, Part 3Conformity evaluation
[3] Moropoulou A, Bakolas A, Bisbikou K. Investigation of the technology of historic mortars. J Cult Herit 1999;1:45.58.
[4] Pavía S, Caro S. An investigation of Roman mortar technology through the petrographic analysis of archaeological material, Constr Build Mater 2008; 22:1807–181.
[5] Piana M, Danzi E. The Catalogue of Venetian external Plasters: Medieval Plasters. In: Scientific Research and Saveguarding of Venice, Venice 2002; p. 65-71.
[6] Armani E. L'indagine sugli intonaci dell'edilizia storica veneziana in AA.VV. Il colore dell'edilizia storica, Bollettino d'arte, Roma 1982, p.37-40.
[7] AA.VV. L´intonaco: storia, cultura, tecnologia. Padova: Libreria Progetto editore; 1985.
[8] Sabbioni C, Bonazza A, Zappia G. Damage on hydraulic mortars: the Venice Arsenal. *J Cult Herit* 2002;3: 83-88.
[9] Pacheco F, Faria J, Jalali S. Some consideration about the use of lime-cement mortars for building conservation purpouses in Portugal: A reprehensible option or a lesser evil?. *Constr and Build Mater* 2012; 30: 488-494.
[10] Papayianni I, Pachta V, Stefanidou M. Analysis of ancient mortars and design of compatible repair mortars: The case study of Odeion of the archaeological site of Dion. Constr Build Mater 2013; 40: 84-92
[11] Maravelaki-Kalaitzaki P, Agioutantis Z, Lionakis E, Stavroulaki M, Perdikatsis V. Physico-chemical and mechanical characterization of hydraulic mortars containing nano-titania for restoration applications, Cement Concrete Comp 2013; 36:33-41.

[12] Moropoulou A, Bakolas A, Moundoulas P. Criteria and methodology for restoration mortars compatible to the historic materials and structures. In Proceedings of the 9th international congress on deterioration and conservation of stone. Venice; 2000, p. 403-412.
[13] Rashad AM. Metakaolin as cementitious material: History, scours, production and composition – A comprehensive overview. Constr Build Mater 2013; 41: Pages 303-318.
[14] Segui P, Aubert JE, Husson B, Measson M. Utilization of a natural pozzolana as the main component of hydraulic road binder. Constr Build Mater 2013; 40:217-223.
[15] Arizzi A, Cultrone G. Aerial lime-based mortars blended with a pozzolanaic additive and different admixtures: A mineralogical, textural and physical-mechanical study, Constr Build Mater 2012; 31:135-143.
[16] Zendri E, Lucchini V, Biscontin G, Morabito ZM. Interaction between clay and lime in "cocciopesto" mortars: a study by 29 Si MAS spectroscopy. Appl Clay Sci 2004; 25(1-2):1-7.
[17] Izaguirre A, Lanas J. Effect of water-repellent admixtures on the behaviour of aerial lime based-mortars, Cement Concrete Res 2009; 39:1095-1104.
[18] Zhang P, Wittmann FH, Zhao TJ. Observation and quantification of water penetration into strain Hardening Cement-based Composites (SHCC) with multiple cracks by means of neutron radiography. Nucl Instrum Methods 2010; A260:414-420.
[19] Lanzón M, Garcia Ruiz PA. Effectiveness and durability evaluation of rendering mortars made with metallic soaps and powdered silicone. Constr Build Mater 2008; 22:2308-2315.
[20] Lanzon M, Garcia-Ruiz PA. Evaluation of capillary water absorption in rendering mortars, made with powdered waterproofing additives. Constr Build Mater 2009;23:3287-3291.
[21] Izaguirre A, Lanas J, Álvarez J. Ageing of lime mortars with admixtures: Durability and strength assessment. Cement Concrete Res 2010; 40: 1081-1095.
[22] Fabric, Wacker silicones SILRES® Lasting protection for Building. www.Wacker.com. [Online] 2011.
[23] Riethmayer S.A. Die metall seifen als Hydrophobierungsmittel. SÖFW 1961; p. 3-6.
[24] Lanzón M, Garrido A, García-Ruiz PA. Stabilization of sodium oleate as calcium oleate in cement-based mortars made with limestone fillers. Constr Build Mater 2011; 25,2:1001-1008.
[25] Izaguirre A, Lanas J, Álvarez JI. Effect of water-repellent admixtures on the behaviour of aerial lime-based mortars, Cement Concrete Res 2009; 39:1095-1104.
[26] Wendler E, Charola AE. Water and its Interaction with Porous Inorganic Building Materials. Proceedings of the Conference " Hydrophobe V, Water repellent treatment of building materials". Aedificatio Publisher 2008;p. 57-74.
[27] Roos M, König F, Stadtmüller S, Weyershausen B. Evolution of Silicone based Water Repellents for Modern Building Protection. Proceedings of the Conference Hydrophobe V, Water repellent treatment of Building materials. Aedificatio Publisher; 2008.
[28] EN 196-1:2005 Methods of testing cement - Part 1: Determination of strength. European Committee for Standardization.
[29] EN 1015-3 Determination of Consistence of fresh mortars (by flow table). European Committee for Standardization.
[30] EN 1015-6:2007 methods of test for mortar for masonry - part 6: determination of bulk density of fresh mortar. European Committee for Standardization.
[31] EN 196-3 Methods of testing cement. Determination of setting time and soundness. European Committee for Standardization.
[32] CNR-ICR NorMaL 4/80 Distribuzione del Volume dei Pori in Funzione del loro Diametro (Italian normative on stone material-Distribution of pores volume vs. their diameter). Commissione Beni Culturali UNI NorMaL
[33] EN 12390-3:2009 Testing hardened concrete. Compressive strength of test specimens. European Committee for Standardization.
[34] EN 12390-5:2009 Testing hardened concrete. Flexural strength of test specimens. European Committee for Standardization.
[35] EN 1015-18:1999 Methods of Test for Mortar for Masonry - Part 18: Determination of Water Absorption Coefficient due to Capillary Action of hardened Rendering Mortar. European Committee for Standardization.
[36] UNI EN 1015-19, Methods of Test for Mortar for Masonry - Part 19: Determination of Water Vapour Permeability of hardened Rendering and Plastering Mortars
[37] DIN 52615 Testing of thermal insulating materials; Determination of water vapour permeability of construction and insulating materials
[38] EN 12370 Natural Stone Test Methods - Determination of Resistance to Salt Crystallisation. European Committee for Standardization.
[39] CNR- ICR NorMaL 13/83 Dosaggio dei sali solubili totali mediante misure di conducibilità (Italian normative on stone material- Determination of the content of soluble salts with conductivity measurments).
[40] Lothenbach B, Le Saout G, Gallucci E, Scrivener K. Influence of limestone on the hydration of Portland cements. Cement Concrete Res 2008;38, 6: 848-860.

[41] Taylor H. F. W. Cement Chemistry. 2nd ed. Oxford: Thomas Thelford; 1997.
[42] Lea M. Chemistry of Cement and Concrete, 4th ed. London: Ed Peter C Hewlett London; 1997.
[43] Donchev I, et al. On the formation of cement phases in the cours of interaction of kaolinite with portlandite. Journal of the university of Chemical Technology and Metallurgy 2010;45,4:391-396.
[44] Sepulcre-Aguilar A, Hernández-Olivares F. Assesment of phase formation in lime based mortars with added metakaolin, portland cement and sepiolite, for grouting of hystoric masonry. Cement Concrete Res 2010; 40, 1: 66-76.
[45] Gualtieri AF, Viani A, Montanari C. Quantitative phase analysis of hydraulic limes using Rietveld method. Cement Concrete Res 2006; 36, 2: 401-406.
[46] Esteves, LP. On the hydration of water-entrained cement–silica systems: Combined SEM, XRD and thermal analysis in cement pastes, Thermochimica Acta 2011; 518: 27-35.
[47] Schwarz N, Neithalath N. Influence of a fine glass powder on cement hydration: Comparison to fly ash and modeling the degree of hydration. Cement Concrete Res 2008; 38:429-436.
[48] Song MG, Kim JY, Kim JD. Effect of sodium stearate and calcium ion on dispersion properties of precipitated calcium carbonate suspensions. Colloid Surf. A-Physicochem. Eng. Asp 2003; 229:75-83.
[49] Wang Z, Wang C, Sheng Y, Hari-Bala, Zhao X, Zhao J. Synthesis of hydrophobic $CaCO_3$ nanoparticles. Mater Lett 2006;60:854–7;
[50] Maravelaki-Kalaitzaki P, Karatasios I, Bakolas A, Kilikoglou V. Hydraulic lime mortars for the restoration of the historic masonry in Crete. Cement Concrete Res 2005; 35:1577–1586.
[51] Lanas J,. Pérez Bernal J, Bello MA, Alvarez Galindo JI. Mechanical properties of natural hydraulic lime-based mortars. Cement Concrete Res 2004; 34:2191-2201.
[52] Lanas J, Sirera R, Alvarez JI. Study of the mechanical behavior of masonry repair lime-based mortars cured and exposed under different conditions. Cement Concrete Res 2006; 36: 961-970.
[53] Biscontin G, Falchi L, et al. Dispersioni acriliche nanometriche e silici colloidali acquose per il consolidamento di materiali porosi. In *Scienza e Beni Culturali.* Arcadia Ricerche, 2011; p. 387-400.
[54] Li W, Wittmann FH, Jiang R, Zhao T, Wolfsehe R. Metal Soaps for the Production of Integral Water Repellent Concrete. Proceedings of the Conference " Hydrophobe VI Rome, Water repellent treatment of building materials". Aedificatio Publisher 2011;145-154.

Tables and Figures

Table 1 Chemical composition of components determined by energy dispersive X-ray fluorescence analysis (- = not present)

	Binder				Admixtures			
	$Ca(OH)_2$		Pozzolana		Silres A		CaSt	
Oxide	At%	Error%	At%	Error%	At%	Error%	At%	Error%
Na_2O	0.3	3	3.7	3	3.4	3	6.2	6
MgO	0.8	6	2.3	2	1.6	3	1.7	13
Al_2O_3	0.1	6	8.9	1	0.8	2	0.2	1
SiO_2	0.3	2	80.4	1	92.8	0	9.0	1
SO_3	0.2	1	0.2	3	1.2	1	0.3	3
K_2O	0.3	1	2.7	1	0.0	2	0.3	2
CaO	97.8	1	1.1	1	0.1	3	82.1	1
Fe_2O_3	-	-	0.5	1	-	-	-	-

Table 2 XRD analysis of the hydration products in pastes HLA, HLsil, HLcas (+++ = high presence; ++ = medium; * = low presence;-= not present)

Time (days)	**1 Halloysite $Al_2Si_2O_5(OH)_4.2H_2O$**			**2 Paraaluminum hydrocalcite $CaAl_2(CO_3)_2(OH)_4.6H_2O$**			**3 Calcium aluminum oxide carbonate hydroxide hydrate $Ca_4Al_2O_6.CO_3.11H_2O$**			**4 Calcium Oxide Carbonate hydrate $3CaO.Al_2O_3CaCO_3.11H_2O$**		
	HLA	**HLSil**	**HLCas**	**HLA**	**HLSil**	**HLCas**	**HLA**	**HLSil**	**HLCas**	**HLA**	**HLSil**	**HLCas**
0	+++	+++	+++	-	-	-	-	-	-	-	-	-
1	+++	+++	+++	+	-	+	-	-	-	-	-	-
2	+++	+++	+++	++	+	++	-	+	+	-	-	-
7	+	+	-	+++	+++	+++	+	++	+	-	-	-
28	-	-	-	++	+++	++	++	+++	+	-	-	-
84	-	-	-	++	++	++	++	++	++	-	-	-
140	-	-	-	+	++	+	++	++	++	+	+	-

Table 3 Total bound water (Tbw), portlandite ($Ca(OH)_2$) and calcite ($CaCO_3$) content of the pastes HLA. HLsil1. HLcas1 at different hydration times obtained from the TG-DTA data

Sample	**Tbw (%)**	**$Ca(OH)_2$ (%)**	**$CaCO_3$ (%)**
	100-350 °C	**400-550 °C**	**650- 800 °C**
HLA 0d	2.7	43.3	1.5
HLA 2d	3.9	41.1	1.6
HLA 7d	5.2	36.4	1.2
HLA 28d	7.2	29.3	1.8
HLsil1 0d	2.8	43.7	1.8
HLsil1 2d	3.4	41.0	3.6
HLsil1 7d	4.8	36.4	2.8
HLsil1 28d	7.2	28.5	1.9
HLcas1 0d	2.8	46.7	2.3
HLcas1 2d	3.9	40.7	5.0
HLcas1 7d	6.1	34.7	2.0
HLcas1 28d	7.1	31.9	0.0

Table 4 Composition of the mortars and characterization of the fresh mortars. The average of three measurements is given with the relative standard deviation.

Mixture name	**Admixture**	**% by mass**	**w/b**	**Slump flow (cm)**	**Density (g/cm^3)**	**Set time (h)**
HLA	-	0	1.250	17.0±0.1	2.09±0.01	35±4
HLsil0.5	Silres A	0.5	1.301	18.3±0.1	1.91±0.01	-
HLsil1	Silres A	1.0	1.196	17.2±0.1	1.89±0.01	65±2
HLsil1.5	Silres A	1.5	1.246	17.5±0.1	1.86±0.01	-
HLcas0.5	Ca Stearate	0.5	1.296	16.8±0.1	2.11±0.01	-
HLcas1	Ca Stearate	1.0	1.296	17.3±0.1	2.06±0.01	40±2
HLcas1.5	Ca stearate	1.5	1.283	17.3±0.1	2.05±0.01	-

Table 5 Structural and mechanical properties of the mortars. Given density and mechanical values are average of 3 measurements with standard deviation

	Apparent density 1 (g/cm^3)	Total porosity (%)	Total open porosity MIP (%)	Modal pore radius MIP (µm)	Compressive strength (MPa)	Flexural strength (MPa)	Elastic modulus tangential (MPa)
HLA	1.77±0.06	32	25	0.1; 9	2.00±0.20	0.37±0.09	1.8±0.1
HLsil0.5	1.55±0.09	40			1.73±0.08	0.32±0.01	1.9±0.4
HLsil1	1.57±0.08	40	29	0.06; 9	2.24±0.07	0.33±0.02	2.6±0.4
HLsil1.5	1.56±0.01	40			2.04±0.09	0.29±0.01	2.2±0.2
HLcas0.5	1.74±0.06	33			2.35±0.08	0.44±0.14	3.1±0.5
HLcas1	1.73±0.05	33	25	0.1; 9	2.00±0.10	0.39±0.02	3.0±0.7
HLcas1.5	1.71±0.08	34			2.06±0.08	0.42±0.02	3.1±0.4

Table 6 Hygric properties of the mortars. Given values are average of 3 measurements with standard deviation

	Capillary coefficient ($g/(m^2 \cdot s^{0,5})$)	Water vapor Permeability $kg/(m^2 \cdot s)$	Water vapor resistance µ	Capillary coefficient after desalination ($g/(m^2 \cdot s^{0,5})$)
HLA	334±19	$6*10^{-7}$±$1*10^{-7}$	11.0±1.0	-
HLsil0.5	0.78±0.08	$8.4*10^{-7}$±$0.5*10^{-7}$	9.0±0.5	1.05±0.07
HLsil1	0.75±0.05	$5.6*10^{-7}$±$0.7*10^{-7}$	14.3±0.7	0.64±0.20
HLsil1.5	0.97±0.04	$5.1*10^{-7}$±$0.5*10^{-7}$	14.1±0.3	0.72±0.01
HLcas0.5	31±7	$5.8*10^{-7}$±$0.6*10^{-7}$	12.7±0.8	67.76±1.29
HLcas1	4.2±0.4	$5.1*10^{-7}$±$0.7*10^{-7}$	13.1±0.9	60.60±1.90
HLcas1.5	2.3±0.3	$5.6*10^{-7}$±$0.5*10^{-7}$	13.0±0.9	28.51±1.13

Table 7 Results of ionic conductivity measurements of samples collected from specimens before and after immersion cycles in sodium sulphate solution. Samples from different depths were collected and measured. Given values are average of 3 measurements with standard deviation

	Conductivity (µs cm^{-1})		
	HLMA	HLMsil	HLMcast
Before	71±6	50±3	102±5
2-1.5 cm	157 ±5	64±5	119±9
1.5-1 cm	146±5	64±5	121±10
1-0.5 cm	154±5	58±5	144±5
0.5-0 cm	209±10	56±2	235±12

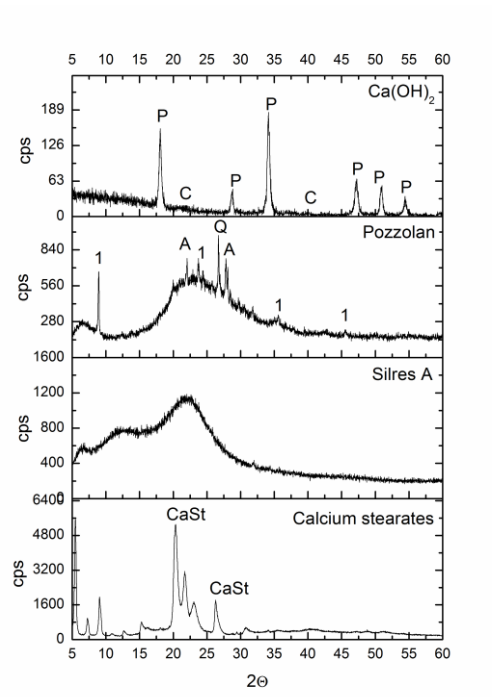

Figure 1 XRD pattern of pozzolana, calcium hydroxide, Silres A (silane) and calcium stearate; P=portlandite; C= calcite; A= albite; Q= quartz; 1=silico aluminate Halloysite

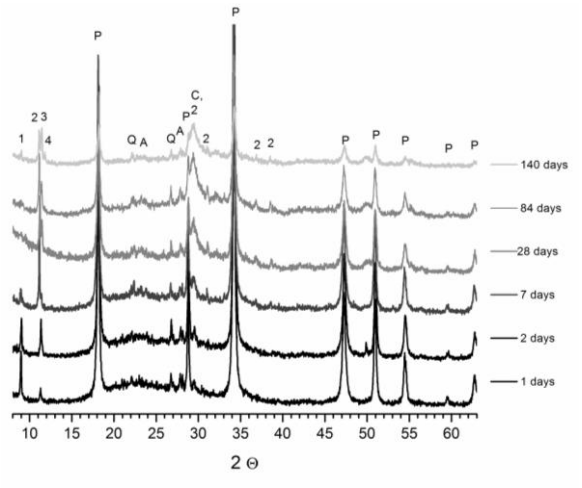

Figure 2 XRD patterns registered for HLA samples at 1, 2, 7, 28, 84 and 140 days. The main peaks of portlandite (P), quartz (Q), albite (A), C-S-H (C), silico-aluminum hydrate (1) and monocarbonates (2, 3, 4) are indicated

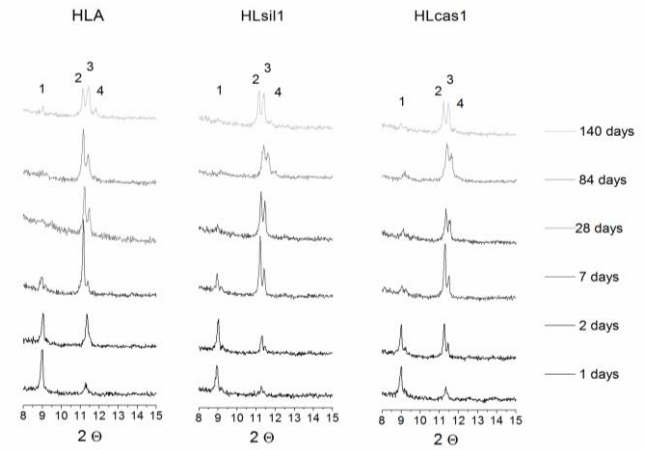

Figure 3 XRD patterns for HLA, HLsil1 and Hlcas1 blends at 1. 2. 7. 28. 84. 140 days (8-15 2theta range). The main peaks of halloysite(1), calcium alluminates (2.3) and C-A-H (4) are indicated.

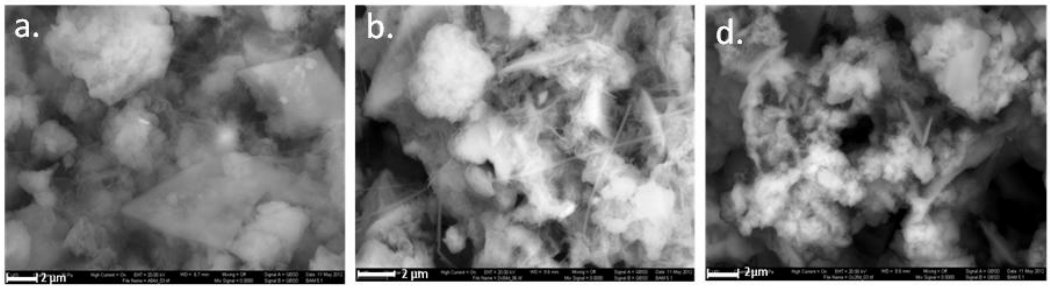

Figure 4 SEM observation of samples cured for 84 days: a. HLA. b, HLsil1, c. HLcas1

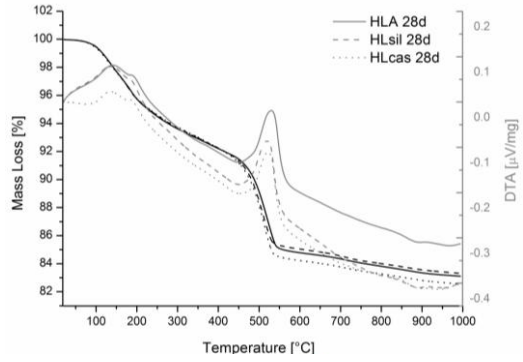

Figure 5 TG-DTA curves of HLA, HLsil and HLcas at 28 days; TG curves as black lines. DTA curves as grey lines

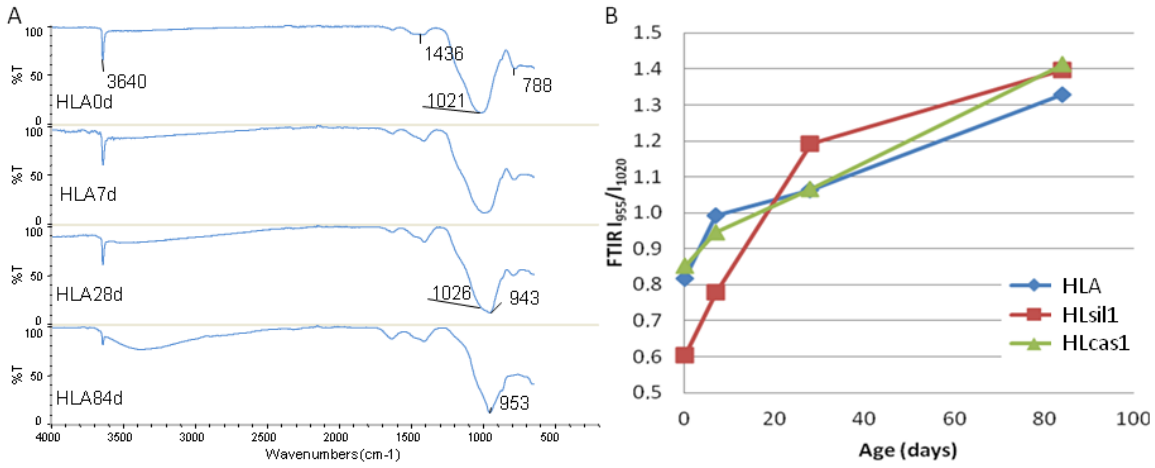

Figure 6 A. FT-IR transmittance spectra of the mixture HLA at 0.7, 28 and 84 days; B. graph of the 955 cm $^{-1}$ and 1020 cm $^{-1}$ peaks intensity ratio versus the curing time.

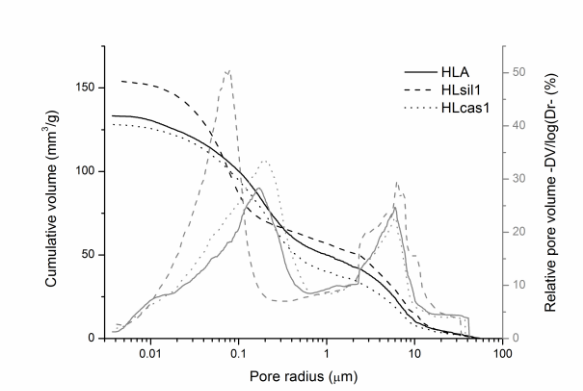

Figure 7 Pore size distributions of mortar mixtures HLA, HLsil1, HLcas1. Cumulative volume as black lines, relative pore volume as grey lines

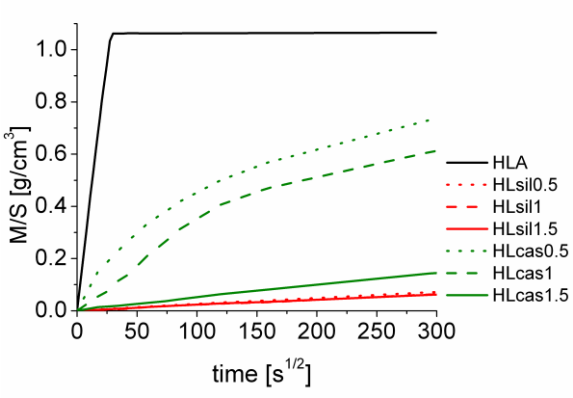

Figure 8 Capillary water absorption

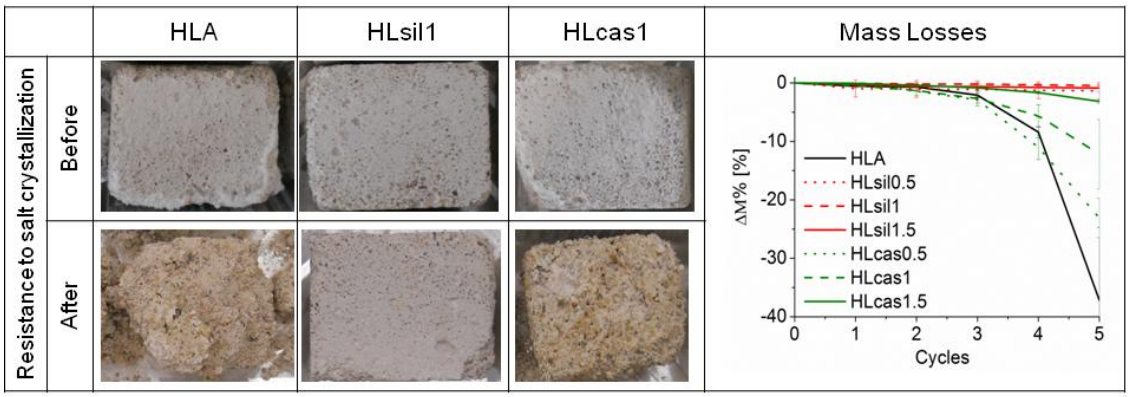

Figure 9 Images of the specimens before and after salt attack and mass loss during salt resistance cycles

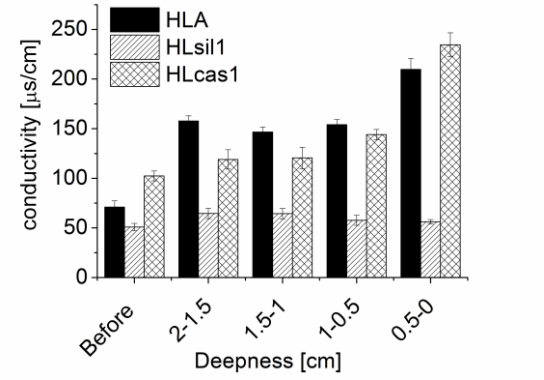

Figure 10 Ionic conductivity of samples collected from specimens before and after immersion cycles in sodium sulphate solution.

Tables and captions

Table 1 Chemical composition of components determined by energy dispersive X-ray fluorescence analysis (- = not present)

	Binder				Admixtures			
	$Ca(OH)_2$		Pozzolana		Silres A		CaSt	
Oxide	At%	Error%	At%	Error%	At%	Error%	At%	Error%
Na_2O	0.3	3	3.7	3	3.4	3	6.2	6
MgO	0.8	6	2.3	2	1.6	3	1.7	13
Al_2O_3	0.1	6	8.9	1	0.8	2	0.2	1
SiO_2	0.3	2	80.4	1	92.8	0	9.0	1
SO_3	0.2	1	0.2	3	1.2	1	0.3	3
K_2O	0.3	1	2.7	1	0.0	2	0.3	2
CaO	97.8	1	1.1	1	0.1	3	82.1	1
Fe_2O_3	-	-	0.5	1	-	-	-	-

Table 2 XRD analysis of the hydration products in pastes HLA, HLsil, HLcas (+++ = high presence; ++ = medium; * = low presence;-= not present)

Time (days)	1 Halloysite $Al_2Si_2O_5(OH)_4.2H_2O$			2 Paraaluminum hydrocalcite $CaAl_2(CO_3)_2(OH)_4.6H_2O$			3 Calcium aluminum oxide carbonate hydroxide hydrate $Ca_4Al_2O_6.CO_3.11H_2O$			4 Calcium Oxide Carbonate hydrate $3CaO.Al_2O_3CaCO_3.11H_2O$		
	HLA	**HLSil**	**HLCas**	**HLA**	**HLSil**	**HLCas**	**HLA**	**HLSil**	**HLCas**	**HLA**	**HLSil**	**HLCas**
0	+++	+++	+++	-	-	-	-	-	-	-	-	-
1	+++	+++	+++	+	-	+	-	-	-	-	-	-
2	+++	+++	+++	++	+	++	-	+	+	-	-	-
7	+	+	-	+++	+++	+++	+	++	+	-	-	-
28	-	-	-	++	+++	++	++	+++	+	-	-	-
84	-	-	-	++	++	++	++	++	++	-	-	-
140	-	-	-	+	++	+	++	++	++	+	+	-

Table 3 Total bound water (Tbw), portlandite ($Ca(OH)_2$) and calcite ($CaCO_3$) content of the pastes HLA. HLsil1. HLcas1 at different hydration times obtained from the TG-DTA data

Sample	Tbw (%)	$Ca(OH)_2$ (%)	$CaCO_3$ (%)
	100-350 °C	**400-550 °C**	**650- 800 °C**
HLA 0d	2.7	43.3	1.5
HLA 2d	3.9	41.1	1.6
HLA 7d	5.2	36.4	1.2
HLA 28d	7.2	29.3	1.8
HLsil1 0d	2.8	43.7	1.8
HLsil1 2d	3.4	41.0	3.6
HLsil1 7d	4.8	36.4	2.8
HLsil1 28d	7.2	28.5	1.9
HLcas1 0d	2.8	46.7	2.3
HLcas1 2d	3.9	40.7	5.0
HLcas1 7d	6.1	34.7	2.0
HLcas1 28d	7.1	31.9	0.0

Table 4 Composition of the mortars and characterization of the fresh mortars. The average of three measurements is given with the relative standard deviation.

Mixture name	Admixture	% by mass	w/b	Slump flow (cm)	Density (g/cm^3)	Set time (h)
HLA	-	0	1.250	17±0.1	2.09±0.01	35±4
HLsil0.5	Silres A	0.5	1.301	18.3±0.1	1.91±0.01	-
HLsil1	Silres A	1	1.196	17.2±0.1	1.89±0.01	65±2
HLsil1.5	Silres A	1.5	1.246	17.5±0.1	1.86±0.01	-
HLcas0.5	Ca Stearate	0.5	1.296	16.8±0.1	2.11±0.01	-
HLcas1	Ca Stearate	1	1.296	17.3±0.1	2.06±0.01	40±2
HLcas1.5	Ca stearate	1.5	1.283	17.3±0.1	2.05±0.01	-

Table 5 Structural and mechanical properties of the mortars. Given density and mechanical values are average of 3 measurements with standard deviation

	Apparent density 1 (g/cm^3)	Total porosity (%)	Total open porosity MIP (%)	Modal pore radius MIP (µm)	Compressive strength (MPa)	Flexural strength (MPa)	Elastic modulus tangential (MPa)
HLA	1.77±0.06	32	25	0.1; 9	2.00±0.20	0.37±0.09	1.8±0.1
HLsil0.5	1.55±0.09	40			1.73±0.08	0.32±0.01	1.9±0.4
HLsil1	1.57±0.08	40	29	0.06; 9	2.24±0.07	0.33±0.02	2.6±0.4
HLsil1.5	1.56±0.01	40			2.04±0.09	0.29±0.01	2.2±0.2
HLcas0.5	1.74±0.06	33			2.35±0.08	0.44±0.14	3.1±0.5
HLcas1	1.73±0.05	33	25	0.1; 9	2.00±0.10	0.39±0.02	3.0±0.7
HLcas1.5	1.71±0.08	34			2.06±0.08	0.42±0.02	3.1±0.4

Table 6 Hygric properties of the mortars. Given values are average of 3 measurements with standard deviation

	Capillary coefficient ($g/(m^2 \cdot s^{0,5})$)	Water vapor Permeability $kg/(m^2 \cdot s)$	Water vapor resistance µ	Capillary coefficient after desalination ($g/(m^2 \cdot s^{0,5})$)
HLA	334±19	$6*10^{-7}$±$1*10^{-7}$	11.0±1.0	-
HLsil0.5	0.78±0.08	$8.4*10^{-7}$±$0.5*10^{-7}$	9.0±0.5	1.05±0.07
HLsil1	0.75±0.05	$5.6*10^{-7}$±$0.7*10^{-7}$	14.3±0.7	0.64±0.20
HLsil1.5	0.97±0.04	$5.1*10^{-7}$±$0.5*10^{-7}$	14.1±0.3	0.72±0.01
HLcas0.5	31±7	$5.8*10^{-7}$±$0.6*10^{-7}$	12.7±0.8	67.76±1.29
HLcas1	4.2±0.4	$5.1*10^{-7}$±$0.7*10^{-7}$	13.1±0.9	60.60±1.90
HLcas1.5	2.3±0.3	$5.6*10^{-7}$±$0.5*10^{-7}$	13.0±0.9	28.51±1.13

Table 7 Results of ionic conductivity measurements of samples collected from specimens before and after immersion cycles in sodium sulphate solution. Samples from different depths were collected and measured. Given values are average of 3 measurements with standard deviation

	Conductivity (µs cm^{-1})		
	HLMA	HLMsil	HLMcast
Before	71±6	50±3	102±5
2-1.5 cm	157 ±5	64±5	119±9
1.5-1 cm	146±5	64±5	121±10
1-0.5 cm	154±5	58±5	144±5
0.5-0 cm	209±10	56±2	235±12

Captions for figures:

Figure 1 XRD pattern of pozzolana, calcium hydroxide, Silres A (silane) and calcium stearate; P=portlandite; C= calcite; A= albite; Q= quartz; 1=silico aluminate Halloysite

Figure 2 XRD patterns registered for HLA samples at 1, 2, 7, 28, 84 and 140 days. The main peaks of portlandite (P), quartz (Q), albite (A), calcite (C), silico-aluminum hydrate (1) and monocarbonates (2, 3, 4) are indicated

Figure 3 XRD patterns for HLA, HLsil1 and Hlcas1 blends at 1. 2. 7. 28. 84. 140 days (8-15 2theta range). The main peaks of silico- aluminate hydrate (1) and monocarbonates (2.3.4) are indicated.

Figure 4 SEM observation of samples cured for 84 days: a. HLA. b, HLsil1, c. HLcas1

Figure 5 TG-DTA curves of HLA, HLsil and HLcas at 28 days; TG curves as black lines. DTA curves as grey lines

Figure 6 a. FT-IR transmittance spectra of the mixture HLA at 0.7, 28 and 84 days; b. graph of the 955 cm $^{-1}$ and 1020 cm $^{-1}$ peaks intensity ratio versus the curing time.

Figure 7 Pore size distributions of mortar mixtures HLA, HLsil1, HLcas1. Cumulative volume as black lines, relative pore volume as grey lines

Figure 8 Capillary water absorption

Figure 9 Images of the specimens before and after salt attack and mass loss during salt resistance cycles

Figure 10 Ionic conductivity of samples collected from specimens before and after immersion cycles in sodium sulphate solution.

Figure 1

Click here to download high resolution image

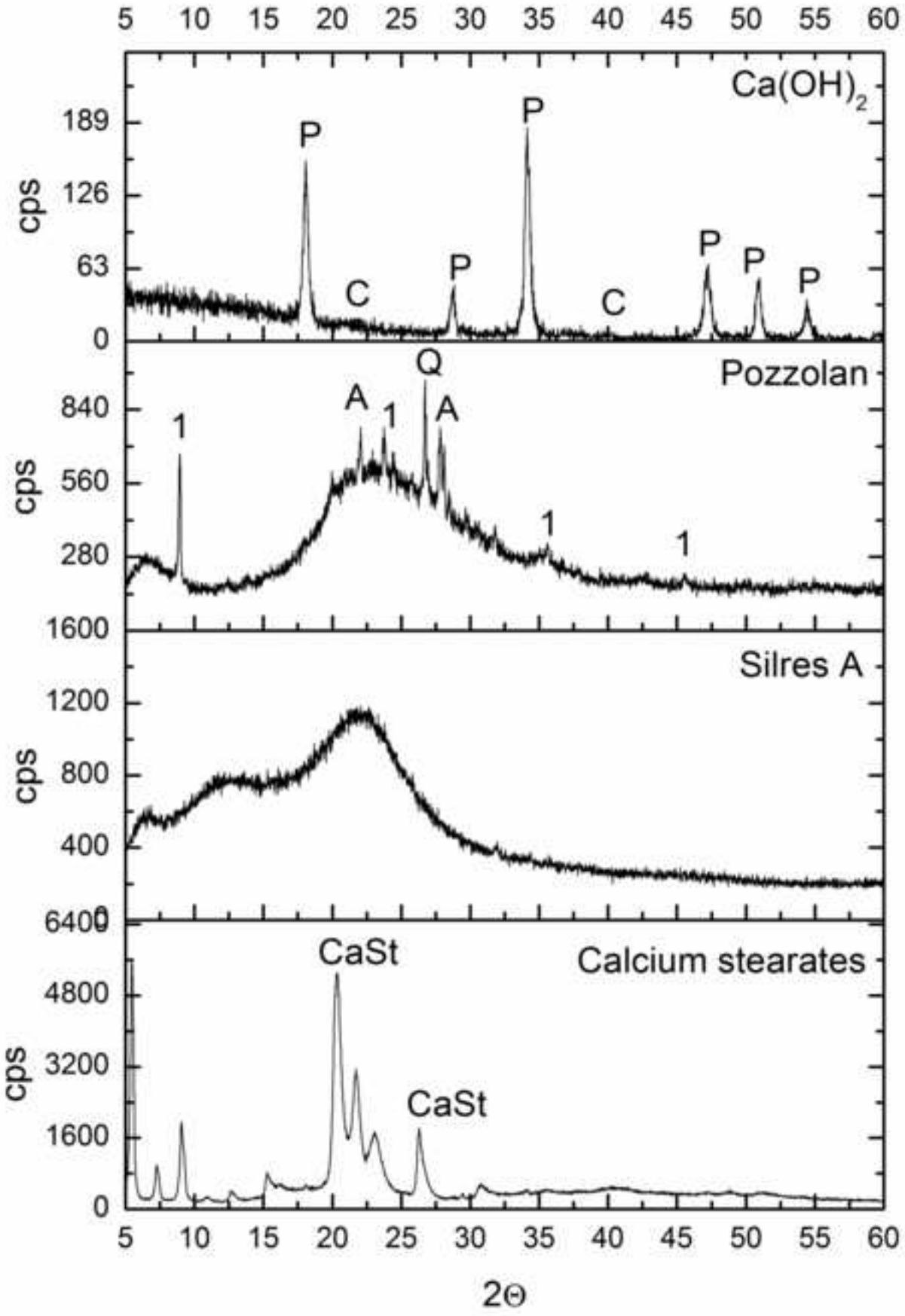

Figure 2

Click here to download high resolution image

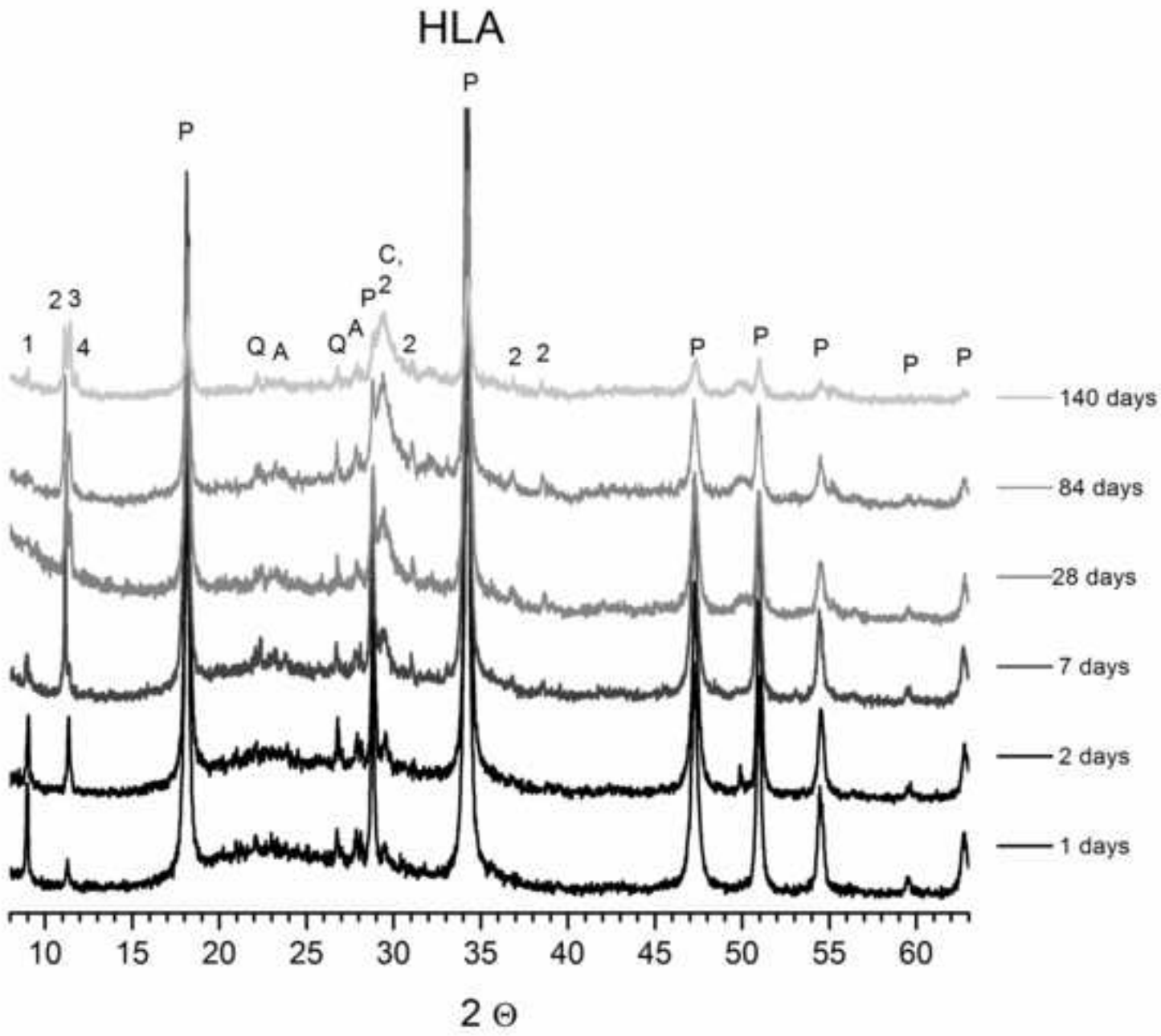

Figure 3

Click here to download high resolution image

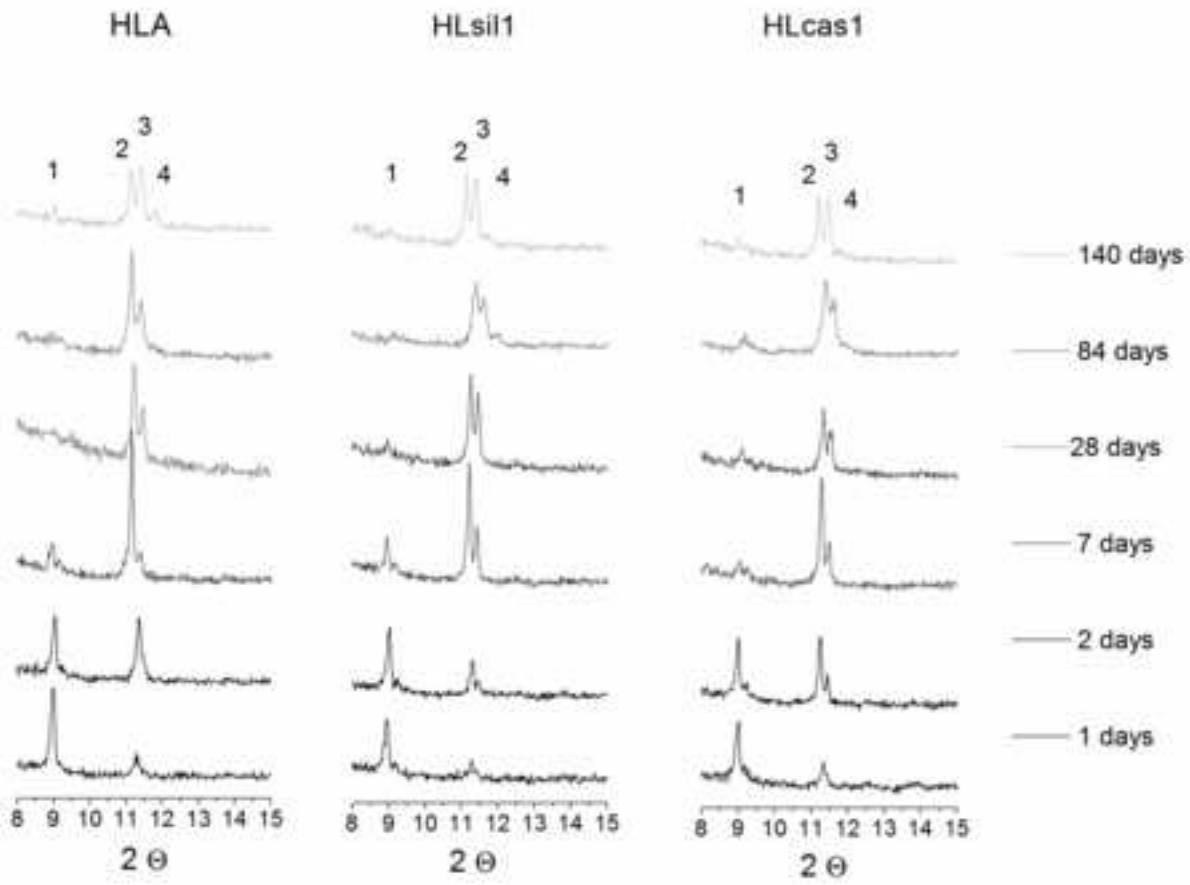

Figure 4

Click here to download high resolution image

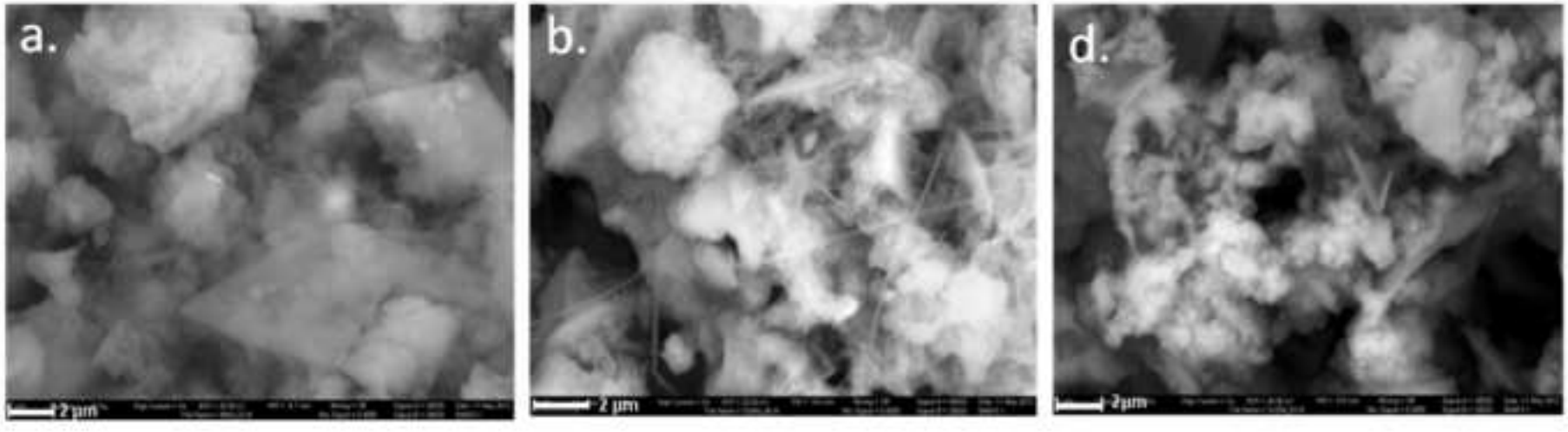

Figure 5

Click here to download high resolution image

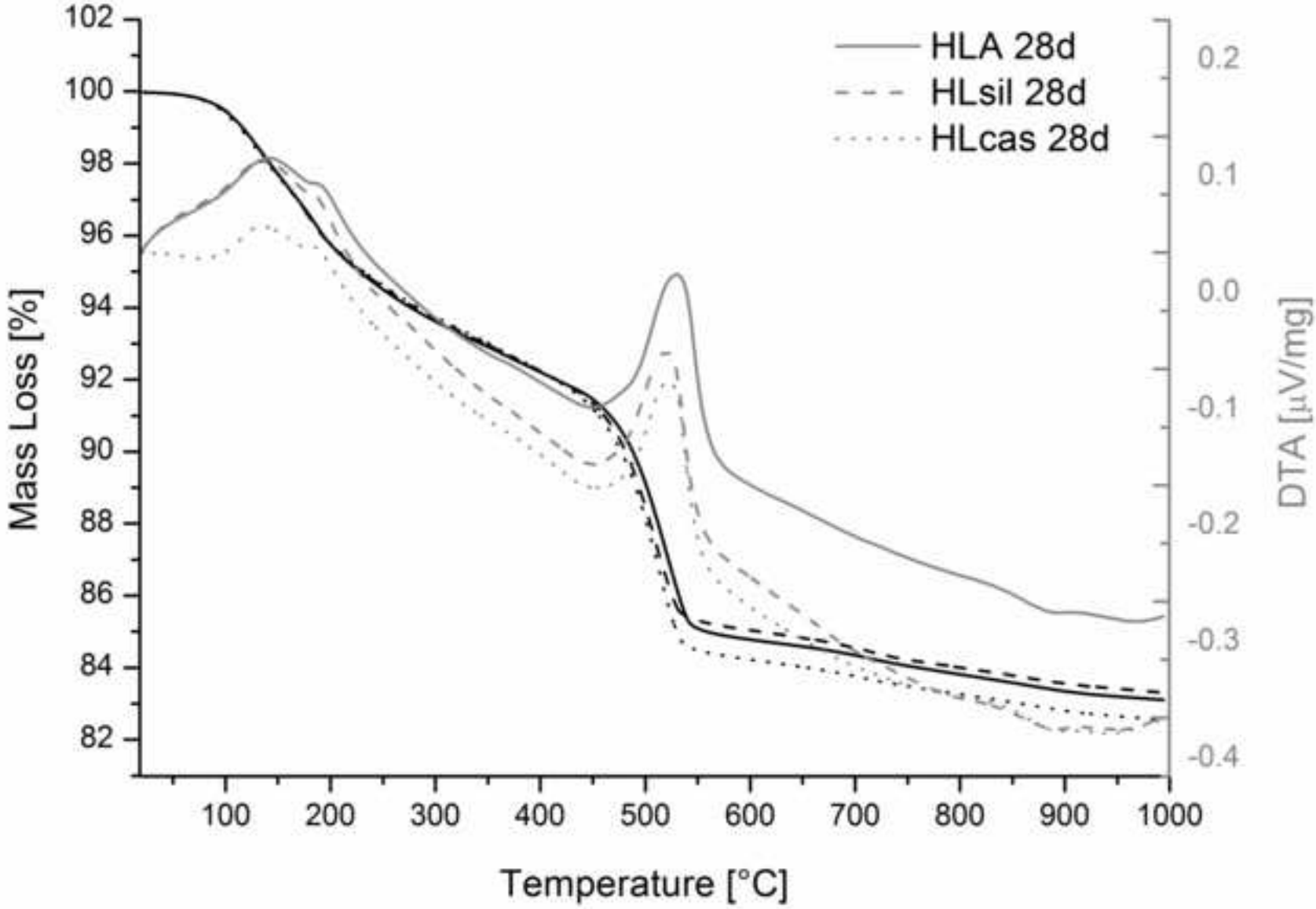

Figure 6

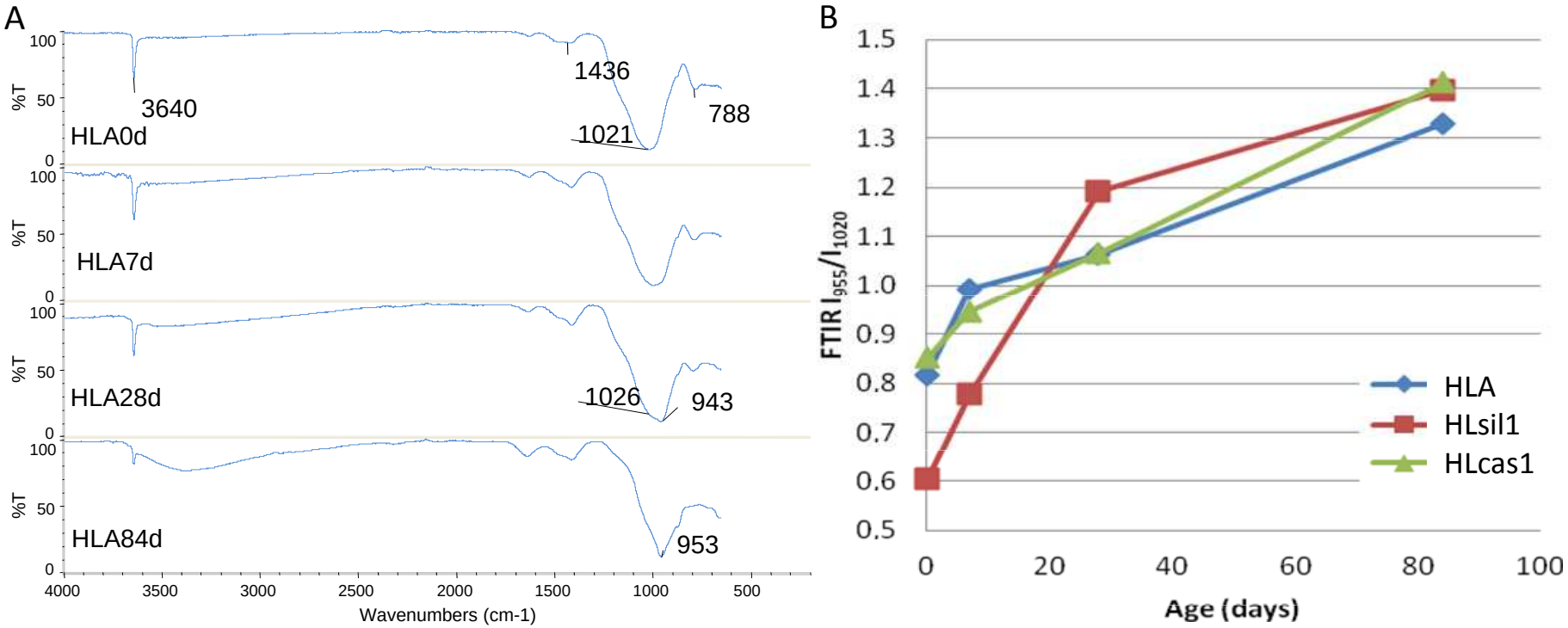
A
100
%T
50
0
3640
1436
788
HLA0d
1021
HLA7d
HLA28d
1026
943
HLA84d
953
4000
3500
3000
2500
2000
1500
1000
500
Wavenumbers (cm-1)
B
1.5
1.4
1.3
1.2
1.1
1.0
0.9
0.8
0.7
0.6
0.5
FTIR I955/I1020
0
20
40
60
80
100
Age (days)
HLA
HLsil1
HLcas1

Figure 7

Click here to download high resolution image

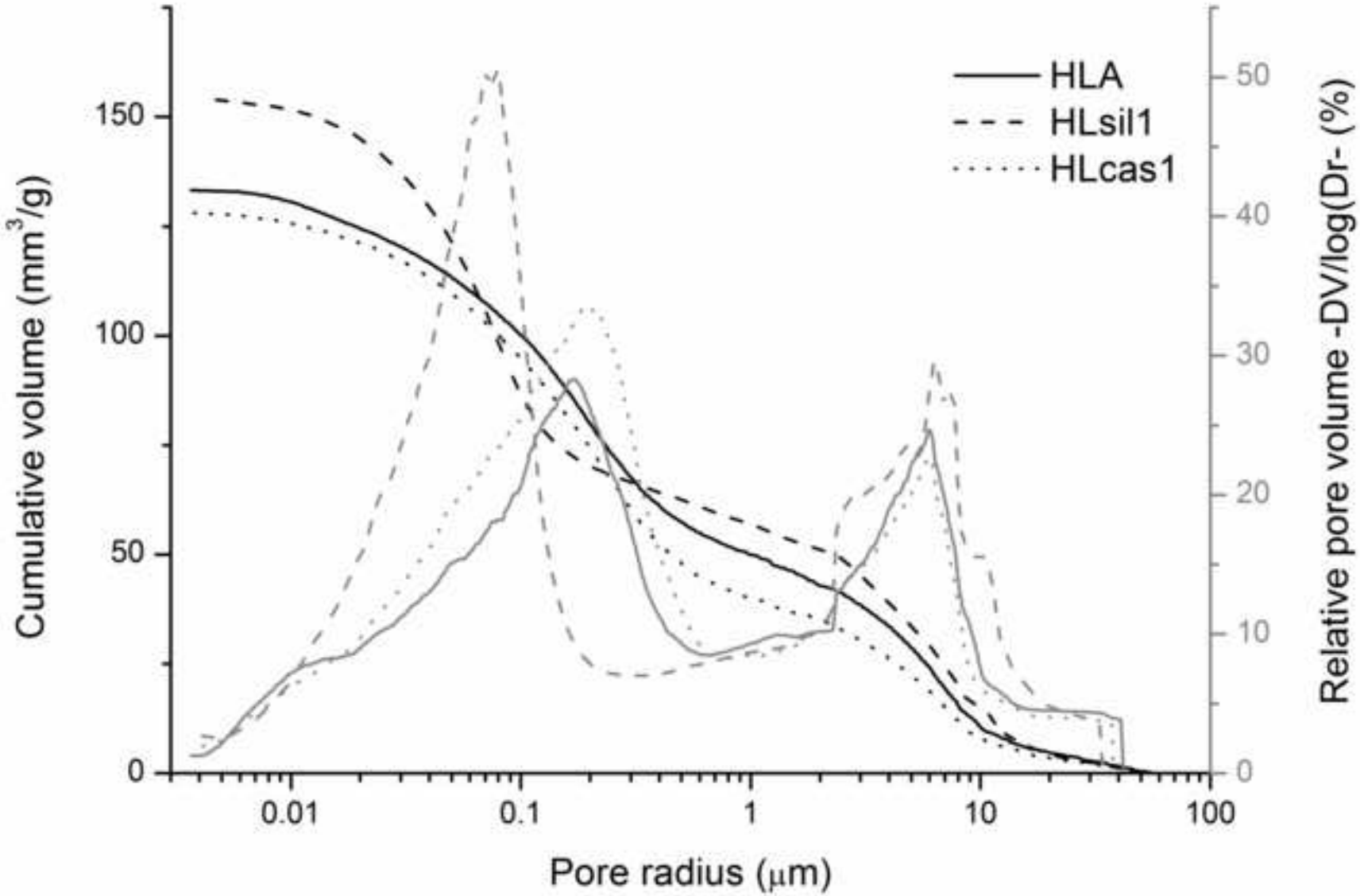

Figure 8

Click here to download high resolution image

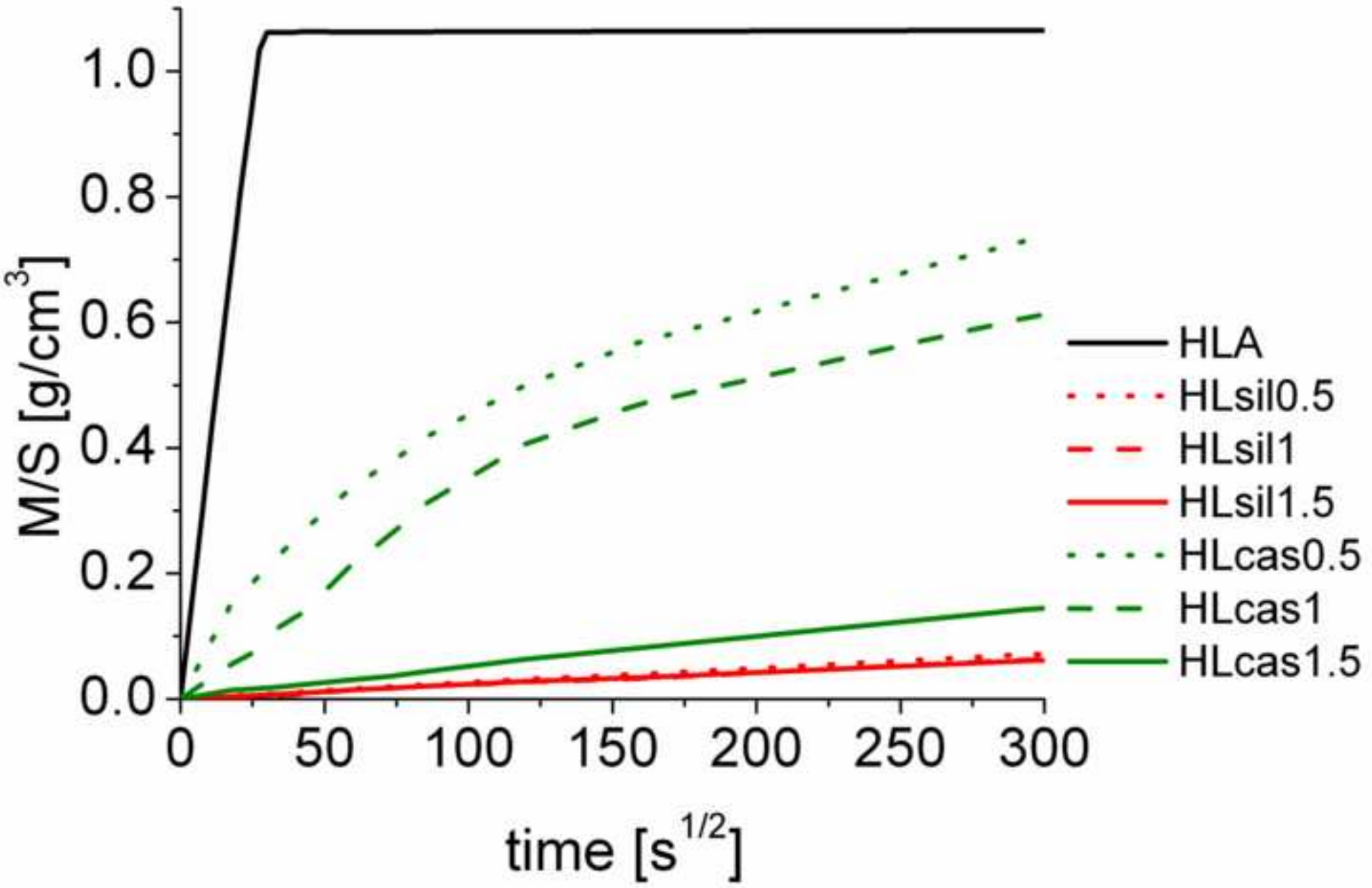

Figure 9

Click here to download high resolution image

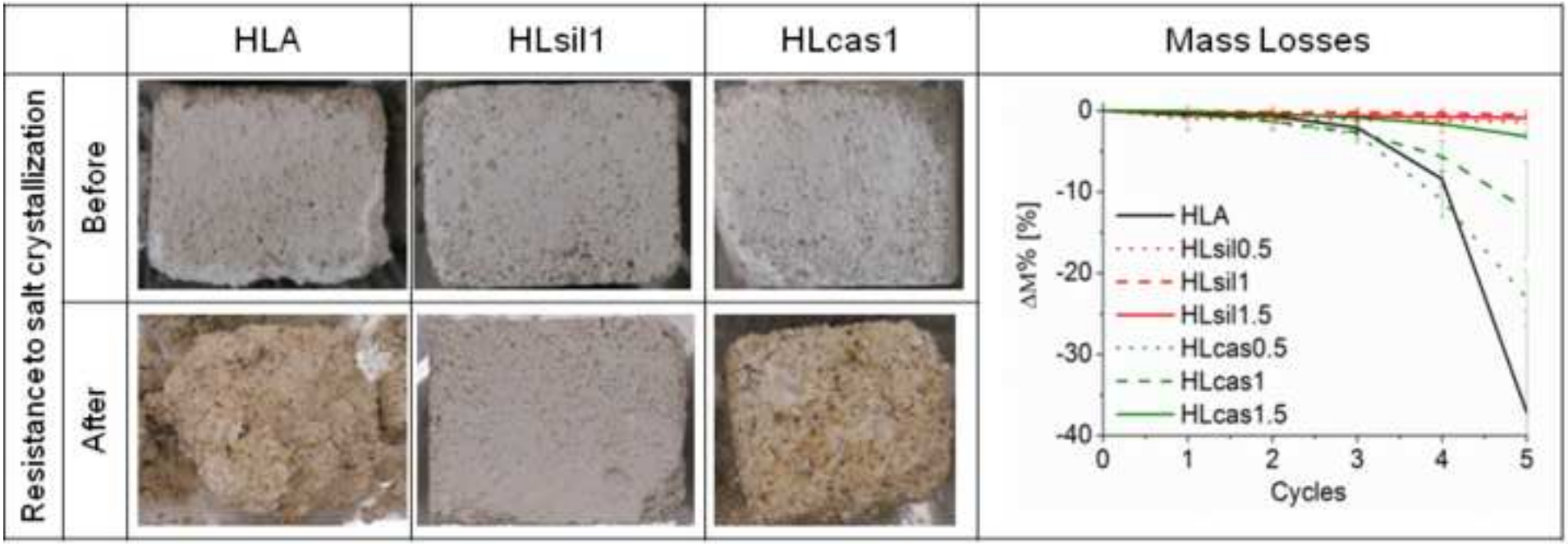

Figure 10

Click here to download high resolution image